Orientational and structural properties of ferroelectric liquid crystal with a broad temperature range in the SmC* phase by ^{13}C NMR, x-ray scattering and dielectric spectroscopy

2009 J. Phys.: Condens. Matter 21 035102

(http://iopscience.iop.org/0953-8984/21/3/035102)

J. Phys.: Condens. Matter **21** (2009) 035102 (8pp) doi:10.1088/0953-8984/21/3/035102

Orientational and structural properties of ferroelectric liquid crystal with a broad temperature range in the SmC* phase by ^{13}C NMR, x-ray scattering and dielectric spectroscopy

Alexej Bubnov[1], Valentina Domenici[2], Věra Hamplová[1], Miroslav Kašpar[1], Carlo Alberto Veracini[2] and Milada Glogarová[1]

[1] Institute of Physics, Academy of Sciences of the Czech Republic, Na Slovance 2, 182 21 Prague 8, Czech Republic
[2] Dipartimento di Chimica e Chimica Industriale, Università degli studi di Pisa, via Risorgimento 35, 56126 Pisa, Italy

E-mail: bubnov@fzu.cz

Received 13 August 2008, in final form 8 October 2008
Published 10 December 2008
Online at stacks.iop.org/JPhysCM/21/035102

Abstract
Thermotropic liquid crystalline materials laterally substituted by a methyl group on the aromatic ring of the alkoxybenzoate unit far from the chiral centre exhibit a very broad temperature range in the ferroelectric smectic C* (SmC*) phase on cooling (including supercooling) with a very high spontaneous polarization (∼210 nC cm^{-2}) and tilt angle (∼43°) at saturation. We are presenting a detailed study of the physical properties of a ferroelectric compound, representative of this category of liquid crystals, by means of solid state ^{13}C-NMR, small angle x-ray scattering, dielectric spectroscopy and optical methods of the tilted SmC*. Values of the spontaneous tilt angle measured optically are compared to those determined from the x-ray data and discussed. In addition, the viscosity has been determined in the SmC* phase by different experimental methods. ^{13}C NMR data allowed us to get information about the degree of orientational order of the SmC* phase and revealed the complete unwinding of the helical axis at the magnetic field of 9.4 T. This result is discussed in the framework of recent publications on the effect of the magnetic field on the supra-molecular structure of the SmC* phase.

1. Introduction

Liquid crystalline (LC) materials with lactate moiety in the chiral part exhibited ferroelectric behaviour in a wide range of temperatures [1, 2]. With the aim of shifting down the temperature interval of the existence of the ferroelectric SmC* phase, a systematic study was done on the preparation of these materials, laterally substituted on the aromatic ring of the alkoxybenzoate unit far from the chiral centre, by chlorine atoms [3], bromine and fluorine atoms [2] or CH_3O and CH_3 groups [3]. LC materials substituted laterally by a methyl group on the aromatic ring of the alkoxybenzoate unit far from the chiral centre exhibit a very broad temperature range in the ferroelectric SmC* phase on cooling (including supercooling) down to room temperature with high spontaneous polarization and tilt angle [3]. Due to the above-mentioned properties these compounds might be interesting from a practical point of view for electro-optical applications as chiral dopants with high spontaneous quantities, namely the spontaneous polarization and spontaneous tilt angle [4]. Among the many interesting technological applications of the last decade, great progress has been made by the display industry: the first high resolution colour displays based on ferroelectric liquid crystals (FLC) were brought on to the Japanese market in 1995 [5]. In the present day the field where smectic FLC materials [6] are

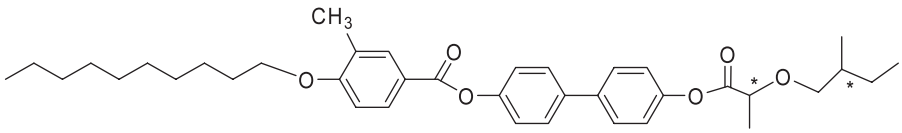

Scheme 1. Molecular structure of the ferroelectric liquid crystal compound M10/**.

well developed is that of optical processing devices, such as spatial light modulators, non-linear optic apparatus, such as waveguides and telecom devices, and the more recent Zeeman laser interferometer used for very accurate measurements of distances, lengths and velocities, based on FLC cells [7].

The supra-molecular structure of the ferroelectric SmC* phase has been widely investigated since its discovery in 1975 [8]. The structure proposed by Meyer for the ferroelectric phase consists of a chiral tilted smectic phase, named chiral smectic C (SmC*), where molecules are arranged in liquid-like smectic layers with each layer possessing an *in-plane* polarization $\vec{P}s$, perpendicular to the molecular 'tilt plane'. The effect of the molecular chirality produces a supra-molecular helical structure: in fact, as reported in [9], the director rotates on moving between layers, maintaining a constant tilt angle and drawing a helix.

The response of this chiral tilted structure to external fields, such as electric and magnetic fields has been the object of several theoretical and experimental studies [5, 10]. Even though the effect of the magnetic field has been studied less, a few works exist [11–13] and the possibility of switching between the unwound and the helical state could potentially be used for technological applications. Quite recently several papers about the effect of the magnetic field in unwinding the supra-molecular structure of several ferroelectric compounds have been published based on ^{2}H NMR studies [14, 15].

^{13}C NMR spectroscopy has been widely used in order to investigate the molecular structure and orientational order of simple liquid crystalline phases, such as the nematic and SmA* ones [16, 17]. In fact, solid state ^{13}C NMR spectroscopy represents not only a complementary method for testing the ^{2}H NMR results, but also the possibility to overcome several practical problems, such as the need for selective deuteration of different fragments of the molecule. On the other hand, due to several difficulties in interpreting and analysing ^{13}C NMR spectra, only a few studies that focus on the ferroelectric phases have been published [18–20]. These works clearly indicate that the support of either ^{2}H NMR spectroscopy or theoretical '*ab initio*' calculations of the chemical shift anisotropy (CSA) is needed in order to overcome the intrinsic problems connected with the application of ^{13}C NMR spectroscopy to such complex systems.

In this work, we have focused on detailed studies of the physical properties of the compound 4′-(2-(-methyl-butoxy)-propanoyloxy-biphenyl-4-yl) 3-methyl-4-nonyloxy-benzoate, denoted here as M10/**. The chemical formula of the studied material is shown in scheme 1. The synthetic details of the compound are reported in [3] with those of the whole series. In the case of M10/**, a lactate moiety with one more chiral centre in a branched alkyl chain was used as a chiral unit; both chiral centres are in (S)-configuration. In this paper, the mesomorphic, structural, orientational and dynamic properties of compound M10/** have been investigated by differential scanning calorimetry (DSC), optical polarizing microscopy, spontaneous quantities measurement, small angle x-ray scattering (SAXS), solid state ^{13}C NMR and dielectric spectroscopy. These results are discussed with the aim of contributing to better understanding of the relationship between the molecular structure and macroscopic physical properties of the chiral liquid crystalline material.

2. Experimental results and discussion

2.1. Mesomorphic properties

The sequence of phases and phase transition temperatures was determined by heating/cooling to/from the isotropic phase, from characteristic textures and their changes observed in the polarizing microscope (NICON ECLIPSE E600POL). The LINKAM LTS E350 heating stage with the TMS 93 temperature programmer was used for temperature control, which enabled temperature stabilization within ±0.1 K. Phase transition temperatures and transition enthalpies were evaluated from differential scanning calorimetry (DSC-Pyris Diamond, Perkin-Elmer 7) on cooling and heating runs at a rate of 5 K min^{-1}. The sample (5 mg) hermetically sealed in an aluminium pan was placed in a nitrogen atmosphere. The temperature was calibrated by extrapolation from the melting points of water, indium and zinc. The enthalpy change was calibrated from the enthalpies of the melting points of water, indium and zinc.

The studied compound M10/** possesses the blue phase (BPI), the cholesteric (N*) phase and subsequently the tilted ferroelectric SmC* phase down to room temperatures. The type of the blue phase has been determined by the characteristic textures and their changes with temperature [21]. The sequence of phases, phase transition temperatures determined on cooling from the isotropic (Iso) phase, and their respective values of enthalpy are shown in table 1. All the phase transitions can be clearly seen on the DSC scan (see figure 1). Interestingly, this compound possesses a wide (partly monotropic) tilted ferroelectric SmC* phase, thermally stable in a range of more than 60 K down to room temperature. Crystallization does not occur below the melting point nor under applied electric fields. A very small peak on the DSC run corresponds to the Iso–BPI phase transition (see the inset in figure 1). For most liquid crystalline compounds the Iso–BPI phase transition is not detectable by means of DSC because of the very small enthalpy.

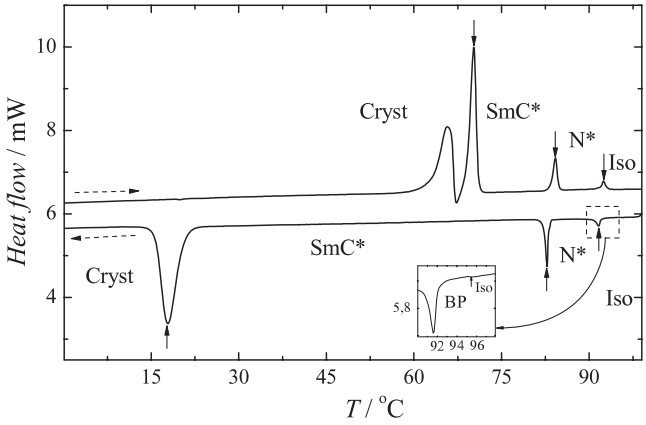

Figure 1. DSC plot of heating/cooling runs as indicated by dashed arrows. Vertical arrows indicate the peaks corresponding to the phase transitions; detected mesophases are indicated. The insert shows the peaks related to the Iso–BPI–N* phase transitions.

Table 1. Phase transition temperatures, T_c, and phase transition enthalpies, ΔH, determined on cooling; melting point, m.p., is determined on heating run.

	T_c (°C)	ΔH (J g^{-1})
m.p.	70	+10.8
Iso–BPI	96	−0.01
BPI–N*	92	−0.4
N*–SmC*	83	−1.6
SmC*–Cryst	18	−15.8

2.2. *Carbon-13 nuclear magnetic resonance*

The high resolution ^{13}C NMR spectra on the bulk liquid crystal M10/** were recorded on a Varian InfinityPlus 400 spectrometer, operating at 100.56 MHz for carbon-13, by using a 5 mm goniometric probe. 1D and 2D solution-state ^{13}C NMR spectra of M10/** in $CDCl_3$ were recorded on a Varian Unity 300 spectrometer, operating at 75.45 MHz for carbon-13, using a standard 5 mm probe. The ^{13}C peak assignments (see scheme 2) in the solution-state and isotropic phase of M10/** compound were aided by the standard techniques DEPT and 2D ^{13}C-^{1}H NMR correlation (HETCOR) experiments. The values of chemical shift, δ^{iso}, in the isotropic phase and the relative assignment are reported in table 2. The ^{13}C peak assignments in the aligned sample were based on the ^{13}C peak assignments of liquid crystals having a similar aromatic core [19, 22, 23, 25]. In the whole mesomorphic temperature range, results of the high resolution solid state ^{13}C NMR experiments on the bulk sample were collected by using the proton-carbon cross polarization (CP) technique with a linear ramp on the carbon channel [27]. Proton decoupling during the ^{13}C signal acquisition was done by the SPINAL-64 pulse sequence [22]. To avoid sample heating the recycle delay between each free induction decay (FID) acquisition was 8 s. The number of scans used was 400. The temperature calibration was made using the known phase transition temperatures of this liquid crystal. The ^{1}H 90° pulse width was 4.2 μs and the temperature gradient across the sample was estimated to be within 1 degree.

Table 2. Components of the chemical shift anisotropy (CSA) tensors for various carbon sites and values of the isotropic component of the chemical shift in the isotropic phase, δ^{iso}.

Carbon no.	σ_{11}	σ_{22}	σ_{33}	δ_{iso}	Reference
1	67.80	169.30	244.10	161.76	[25]
2	17.60	140.60	206.60	120.75	[19]
2′	17.60	140.60	206.60	110.14	[19]
3	45.20	157.20	221.20	132.50	[19]
3′	45.20	157.20	221.20	130.10	[19]
4	20.50	142.50	228.50	127.03	[19]
6	77.00	154.00	237.00	150.68	[19]
7	30.00	149.30	183.00	121.65	[23]
9	14.50	147.40	219.30	138.39	[19]
10	14.50	147.40	219.30	137.82	[19]
11	27.60	135.60	223.60	128.12	[22]
12	30.00	149.30	183.00	122.17	[23]
13	77.00	154.00	237.00	149.90	[22]

Figure 2 shows a series of static CP-SPINAL ^{13}C NMR spectra obtained in the bulk for the ferroelectric M10/** compound as a function of temperature. The sample was aligned in the magnetic field by cooling from the isotropic phase down to the crystalline phase. In the range of stability of the BPI and N* phases, the ^{13}C NMR spectrum is characterized by broad and not well defined peaks (see for instance the aromatic region in the range of 100–150 ppm in figure 2). In fact, on the one hand, the CP-SPINAL technique is not effective in the presence of high mobility and low viscosity, on the other hand, the BPI phase has an isotropic structure and the N* phase is characterized by a cylindrical distribution of orientations. However, from the change in the line-shape, both in the aromatic (from 100 to 150 ppm) and the aliphatic (from 10 to 80 ppm) regions, it is possible to distinguish between these two phases, as shown in figure 2. At the phase transition between the N* and SmC* phases, the observed ^{13}C chemical shifts, δ^{obs}, of the aromatic carbons increase markedly and those of the aliphatic carbons decrease slightly (namely, upfield shifts). This fact is typical of ordered phases, such as the SmA* (paraelectric orthogonal smectic A* phase) one, but it is not expected in the SmC* phase, in which the helical structure usually orients with the helical axis, **h**, and the local phase director, **n**, parallel and tilted with respect to the magnetic field, **H**. For the compound under investigation, the increase of aromatic chemical shifts on the temperature decrease is due to the total unwinding of the helical structure, so that the local phase director **n** is parallel, and the normal ***l*** to the layer is tilted with respect to **H** [14, 15, 18] (see scheme 3).

This means that the NMR magnetic operating field of 9.4 T is higher than the critical field, H_c, and able to unwind the helical structure. This phenomenon has been observed in other chiral smectogens [14, 15] with a similar chemical structure, in which the critical field H_c was found to be in the range of 2–20 T. As a consequence of the total unwinding of the SmC* helical structure, the tilt angle of the phase cannot be determined from the analysis of the temperature variation of chemical shifts.

The assignment of ^{13}C peaks of the aromatic core in the SmC* phase of M10/**, seen in figure 3, was aided by comparison with other smectogens with a similar molecular

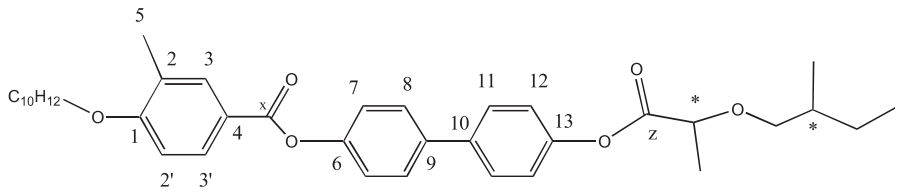

Scheme 2. Molecular structure of M10/** with indicated carbon site labels for the aromatic and COO (carboxyl) carbons.

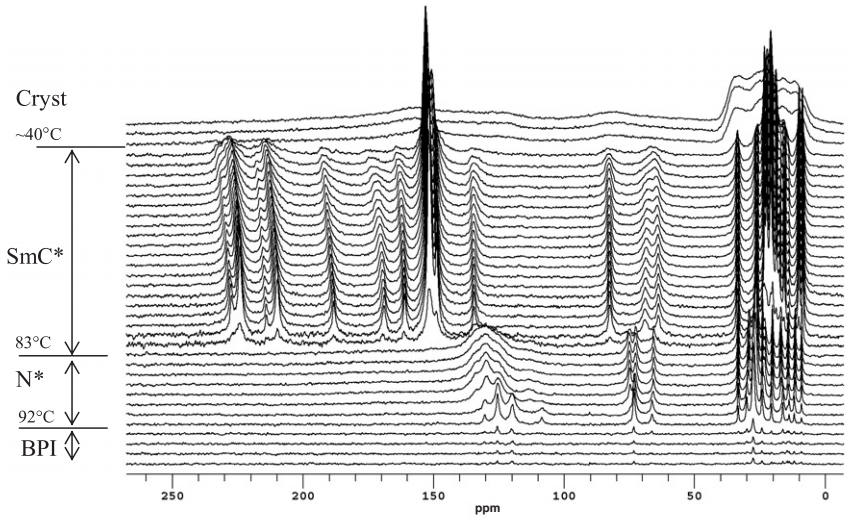

Figure 2. Series of static ^{13}C NMR spectra recorded over the whole mesomorphic temperature range of the M10/** compound by using the CP-SPINAL technique. Mesophases and phase transition temperatures are indicated. Note that the crystalline phase occurs at about 40 °C, thus indicating a supercooled crystallization.

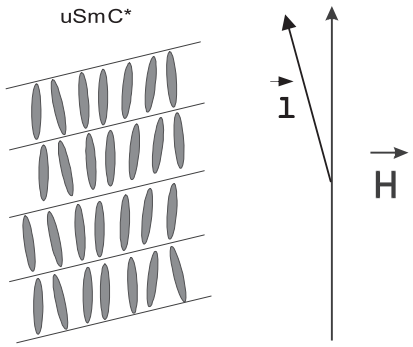

Scheme 3. Representation of the unwound SmC* phase (denoted by uSmC*) in presence of a magnetic field, $\vec{H}$, $\vec{l}$ indicates the normal to the smectic layers.

structure available in the literature [19, 23–26]. However, as it clearly follows from figure 3, several carbon signals completely overlap with each other (such as carbons 9 and 10, 7 and 12, 8 and 11) and the assignment in the SmC* phase of some signals is not straightforward.

For these reasons the analysis of the chemical shift anisotropy (defined as $\delta^{\text{aniso}} = \delta^{\text{obs}} - \delta^{\text{iso}}$, to determine the values of the local orientational order parameters, namely S_{zz} and $\Delta_{\text{biax}} = S_{xx} - S_{yy}$) can be performed considering only a restricted data-set and by fixing the values of the components of the chemical shift anisotropy (CSA) tensor σ_{ii} according to the literature (see table 2, [19, 22–24, 27]). The following equation was used by assuming a uniaxial symmetry of the molecular fragments under study (the phenyl and biphenyl moieties):

$$\begin{aligned}\delta^{(j)} &= \delta^{(j)}_{\text{iso}} \\ &+ \tfrac{2}{3}S_{zz}\left[P_2(\cos\beta^{(j)})(\sigma^{(j)}_{33} - \sigma^{(j)}_{22}) + \tfrac{1}{2}(\sigma^{(j)}_{22} - \sigma^{(j)}_{11})\right] \\ &+ \tfrac{1}{3}(S_{xx} - S_{yy})\left[\sigma^{(j)}_{11} - (\cos^2\beta^{(j)})\sigma^{(j)}_{22} - (\sin^2\beta^{(j)})\sigma^{(j)}_{33}\right]\end{aligned}$$

where $\beta^{(j)}$ is the polar angle for the $\sigma^{(j)}_{ij}$ of the jth carbon in the fragment frame (x_p, y_p, z_p). The nominal values $\beta^{(j)}$ of 60° and 0° are used for the protonated (labelled as 2, 3, 2′, 3′, 7, 8, 11 and 12 in scheme 2) and quaternary (labelled as 'x', 'z', 1, 4, 6, 9, 10 and 13 in scheme 2) carbons, respectively. The calculated average values of the local order parameters S_{zz} for two aromatic fragments (with z being along the *para* axis of the aromatic moiety) are 0.87 and 0.78 for the biphenyl and phenyl fragments, respectively. No sensible temperature dependence has been observed. The average values of the fragment biaxiality are 0.06 and 0.18 for the biphenyl and phenyl moieties, respectively. In both cases, the error is about ±10%. The order parameters as well as the chemical shifts remain constant within the whole temperature range of stability of the SmC* phase (see figure 3). This is in a good agreement with the other physical properties measured in the SmC* of M10/**, as shown in the following paragraphs.

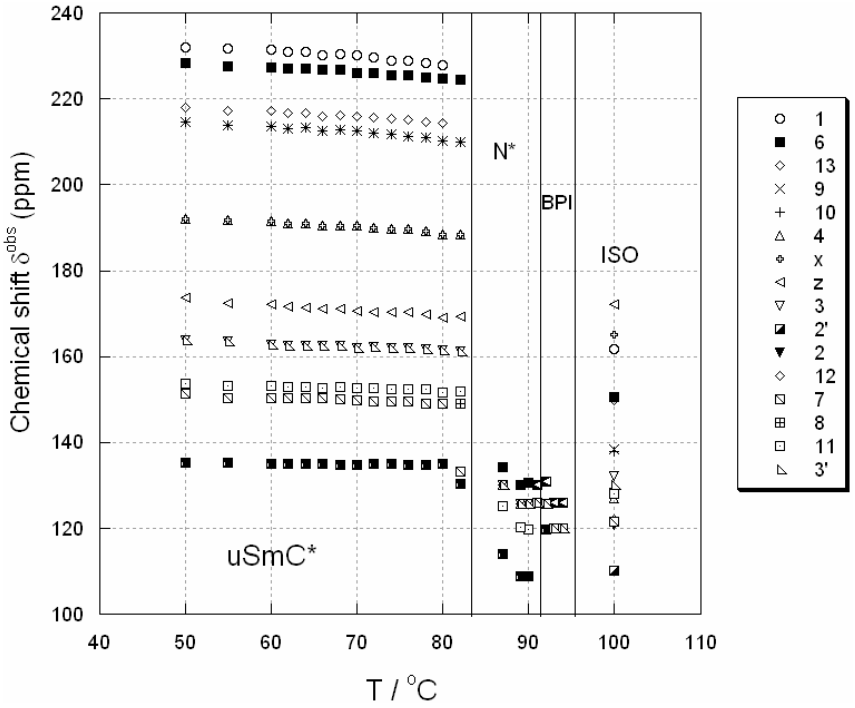

Figure 3. Temperature dependence of the chemical shift δ^{obs} of the aromatic and quaternary carbons of compound M10/** according to scheme 2, with a tentative assignment. Phase transitions are also shown.

2.3. Small angle x-ray scattering (SAXS)

The SAXS studies have been performed with Ni-filtered Cu Kα radiation (wavelength $\lambda = 1.5418$ Å). SAXS data for non-aligned samples (filled into Mark capillary tubes of 0.7 mm diameter) were obtained using a Kratky compact camera (A. Paar) equipped with a temperature controller (A. Paar) and a one-dimensional electronic detector (M. Braun)—the temperature was controlled to within 0.1 K.

Temperature dependence of the layer spacing, d, and the related intensity of the scattered signal of the SAXS studies are shown in figure 4 within the whole temperature range of the tilted ferroelectric SmC* phase. The intensity of the scattered signal slightly increases on cooling due to the increase of the smectic order. However, a decrease in d values on cooling is due to (i) the increasing order of the long molecular axes inside the plane of the smectic layers and (ii) a slight increase of the tilt angle of molecules. For the studied material the average lateral intermolecular distance has been determined: 4.9 Å in the N* phase (at $T = 90\,^{\circ}$C) and 4.6 Å in the SmC* phase (at $T = 76\,^{\circ}$C) [28] indicating the increase of the close packing of molecules on cooling.

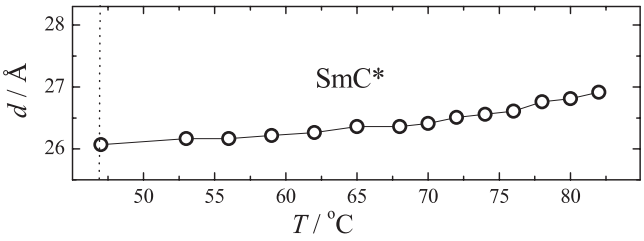

Figure 4. Small angle x-ray scattering studies: temperature dependence of the smectic layer spacing $d(T)$. The dotted lines limit the temperature range of the SmC* phase.

2.4. Spontaneous polarization and tilt angle

Values of the spontaneous polarization, P_s, have been evaluated from the $P(E)$ hysteresis loop detected during P_s switching in the ac electric field E of frequency 60 Hz. Values of the spontaneous tilt angle, θ_s, have been determined optically from the difference between the extinction positions of crossed polarizers under dc electric fields of opposite polarities ± 40 kV cm^{-1}.

In the upper limit of the SmC* phase the values of the spontaneous polarization and spontaneous tilt angle are rather high, which is in accordance with the first order N*–SmC* phase transition. Close below the N*–SmC* phase transition, spontaneous polarization slightly increases and reaches relatively high values up to 210 nC cm^{-2} at saturation (see figure 5(a)). The spontaneous tilt angle measured optically slightly increases on cooling from about 40° (close below N*–SmC* phase transition) and reaches about 43° (see figure 5(b)). In addition, a tilt angle θ_{SAXS} has been calculated from the layer spacing data and the length of the M10/** molecule. The length calculated for the most extended conformer using the MOPAC/AM1 method is $L = 34$ Å. The values of θ_{SAXS} are slightly smaller than those measured optically (see figure 5(b)). This difference might occur due to the fact that each method used for the tilt determination is appropriate for different structure elements. The electro-optical method determines the mean orientation of the molecular core, which defines the optical axis, while

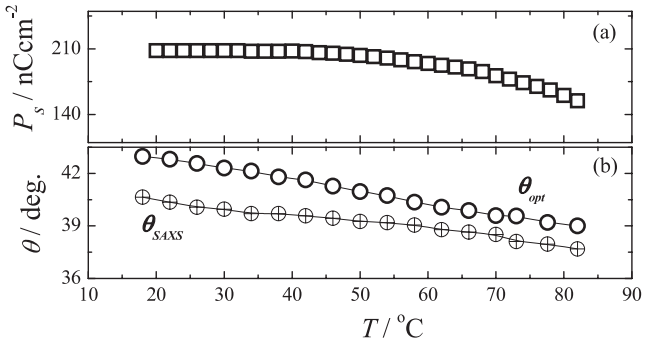

Figure 5. Temperature dependence of: (a) the spontaneous polarization $P_s(T)$ and (b) the tilt angles: $\theta_{opt}(T)$ and $\theta_{SAXS}(T)$.

the SAXS method detects the spatial period of the molecular arrangement [29].

2.5. Dielectric spectroscopy

Frequency dispersion of the complex permittivity $\varepsilon^*(f) = \varepsilon' - i\varepsilon''$ was measured on cooling using a Schlumberger 1260 impedance analyzer in the frequency range of 1 Hz–1 MHz on a 1.8 μm thick sample cell. The frequency dispersion data were analysed within the temperature range of the SmC* phase using the Cole–Cole formula for the frequency dependent complex permittivity:

$$\varepsilon^* - \varepsilon_\infty = \frac{\Delta\varepsilon}{1 + (if/f_r)^{(1-\alpha)}} - i\frac{\sigma}{2\pi\varepsilon_0 f^n},$$

where f_r is the relaxation frequency and $\Delta\varepsilon$ is the dielectric strength of the mode, α is the distribution parameter of the relaxation times, ε_o the permittivity of a vacuum, ε_∞ the high frequency permittivity and n is the parameter of fitting. The second term on the right-hand side of the equation is used to eliminate the low frequency contribution to ε'' from the dc conductivity σ.

A 3D plot of the dielectric absorption spectrum $\varepsilon''(f, T)$ with one mode in the SmC* phase is shown in figure 6. The results of fitting the temperature dependence of the relaxation frequency, f_r, the dielectric strength, $\Delta\varepsilon$, and the distribution parameter of the relaxation times α are shown in figure 7. There is a decrease in the dielectric strength and relaxation frequency while approaching the low temperature limit of the SmC* phase. Increase of the viscosity while approaching room temperature is the source of the relaxation frequency decrease. The decrease in the distribution parameter of the relaxation times α indicates that at lower temperatures the relaxation process is close to pure Debye behaviour ($\alpha = 0$).

2.6. Viscosity

In the ferroelectric SmC* phase, generally two viscosities are defined, the soft mode viscosity associated with the change of the tilt magnitude, which describes the tilt amplitude fluctuations and the Goldstone mode rotational viscosity related to the rotation of the director about the layer normal [30]. These viscosities can be calculated from the

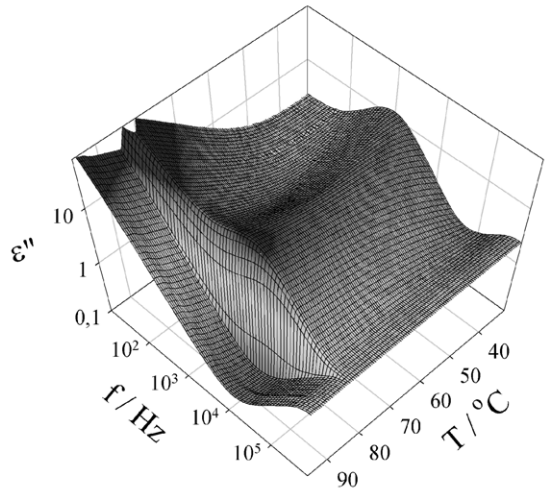

Figure 6. 3D plot of the dielectric absorption spectrum $\varepsilon''(f, T)$ measured on a planar 1.8 μm thick sample cell.

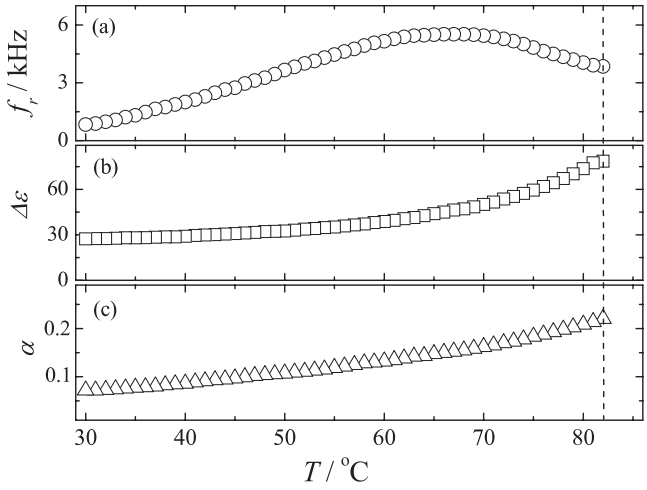

Figure 7. Temperature dependence of the relaxation frequency, f_r (a), dielectric strength, $\Delta\varepsilon$ (b), and distribution parameter of the relaxation times, α (c). The dashed line indicates the temperature of the phase transition to the SmC* phase.

relaxation frequencies of the respective modes. The soft mode is negligible in the studied compound, it could be detected only in close vicinity of the SmA*–SmC* phase transition. The rotational viscosity related to the Goldstone mode can be determined from the dielectric spectroscopy data using the equation [31]:

$$\gamma_\varphi^d = \frac{1}{4\pi\varepsilon_o}\frac{1}{\Delta\varepsilon f_r}\left(\frac{P_s}{\theta_s}\right)^2$$

where ε_o is the permittivity of a vacuum, f_r is the relaxation frequency of the Goldstone mode, $\Delta\varepsilon$ is the dielectric strength of the mode, P_s is the spontaneous polarization and θ_s is the tilt angle of the molecules. Also, a viscosity related to the rotation of molecules about the normal to the layer during ferroelectric switching, γ_φ, can be defined and calculated by analysing the current response on an applied triangular driving voltage. It is

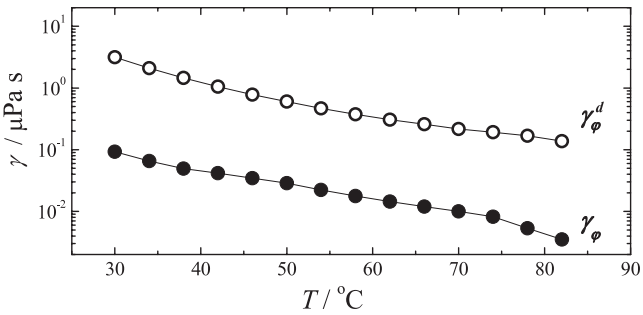

Figure 8. Temperature dependences of the viscosity γ_ϕ obtained from the polarization switching, and γ_φ^d obtained from the dielectric spectroscopy as indicated.

given by [30]

$$\gamma_\varphi = \frac{SP_s^2 E_m}{I_m},$$

where I_m is the current peak value, E_m the corresponding electric field and S is the active electrode area of the sample cell. Comparison of the temperature dependence of the viscosity in the SmC* phase related to (i) small fluctuations in the direction of the azimuthal angle detected by dielectric spectroscopy under a relatively small applied electric field (γ_φ^d) and (ii) polarization switching under a strong applied electric field (γ_φ) are presented in figure 8. Both viscosities increase when approaching the room temperature, the former being more than by one order lower.

3. Summary of the results and conclusions

The orientational order, structural and dynamics properties of the liquid crystalline material, laterally substituted by a methyl group on the aromatic ring of the alkoxybenzoate unit far from the chiral centre, has been studied. This compound exhibits a wide smectic C* phase, stable on cooling (including supercooling) in a range of more than 60 K.

The spontaneous polarization reaches high values up to 210 nC cm^{-2} at saturation. Rotational viscosity related to the fluctuations in the tilt direction has been determined and exhibits the increase on cooling. The spontaneous tilt angle measured optically, slightly increases on cooling from about 40° (close below the N*–SmC* phase transition) and reaches about 43° at the low temperature limit of the SmC* phase. Due to high values of the tilt angle the studied compound can be called a ferroelectric orthoconic (tilt angle is 45°) material [32].

In the tilted SmC* phase the layer spacing was found to be about 27 Å, close below the phase transition from the N* phase. On cooling it slightly decreased down to 26 Å. For calculation of the tilt angle from the SAXS measurements, the length of the most extended molecule conformer 34 Å found by the semiempirical MOPAC method was used. Values of θ_{opt} were found slightly higher than those calculated from the SAXS data. This difference follows from the different sensitivity of the methods used: the optical method determines the mean orientation of the molecule core, which defines the optical properties, while the SAXS method is related to the spatial period of the molecular arrangements [29, 33, 34].

The helical structure of the SmC* phase is partially unwound as the dechiralization lines are rare and irregular. However, a strong relaxation mode, namely the Goldstone mode, has been detected within the whole range of the ferroelectric SmC* phase by dielectric spectroscopy.

Two rotational viscosities, one related to the polarization switching and the other related to the molecular fluctuations in the azimuthal direction, have been determined, the former being more than one order higher.

High resolution ^{13}C NMR spectroscopy on the bulk sample allowed us to check the mesophase transitions by the change of both the line-shape and the temperature dependence of the carbon-13 chemical shifts. Sensible changes in the line-shape and broadening effects have been observed at the transition between the BPI and N* phases, and a big jump at the transition between the N* and SmC* phases. This evident change in the recorded ^{13}C NMR spectra reflects the formation of a highly ordered phase, whose order parameters, determined locally for the aromatic phenyl and biphenyl moieties from the chemical shift anisotropy, reach values of 0.72 and 0.87, respectively, without any gradualness and continuity with respect to the previous high temperature mesophases. The order parameters, as well as the chemical shift anisotropies, have a very small temperature dependence within the range of stability of the SmC* phase. Similar behaviour is found for the other measured physical properties, such as the tilt angle obtained by optical and x-ray measurements, which reaches the saturated value in a few degrees of temperature. The occurrence of a jump in the orientational order parameter, as well as in the spontaneous polarization and tilt angle of the molecules at the N*–SmC* phase transition is quite typical for ferroelectric mesogens that do not have less ordered smectic phases, such as the SmA* one [18]. This discontinuity of the orientational order is a consequence of the strongly first-order transition.

Another important phenomenon revealed by NMR is the total unwinding of the helical supra-molecular structure of M10/** in presence of the magnetic field of 9.4 T. It is the first time when such behaviour has been observed for a compound not exhibiting the SmA* phase at higher temperatures. In fact, we know at least four cases [14, 15, 35] in which the helical structure of the SmC* phase is partially or totally unwound by a magnetic field parallel to the helical axis, but all of them present the SmA* phase above the SmC* phase. By comparing the case of M10/** with other ferroelectric smectogens [14, 15, 23, 31, 36] some considerations may arise: (i) the value of the critical magnetic field H_c differs from one smectogen to another being related to some physical properties specific of the compound; (ii) the supra-molecular structure is typically unwound by a magnetic field parallel to the helical axis in the range of 2–20 T. The compound studied in this work represents a good candidate for better exploration of the properties of the SmC* phase in the presence of a magnetic field and to test the theoretical model of the SmC* response to magnetic fields [14, 15], because of its large stable temperature range. With this objective, the next step of this research will be the synthesis of a selectively deuterated compound to be studied by means of ^{2}H NMR. There is a probability that

at magnetic fields lower than 9.4 T used for ^{2}H NMR, the structure of the SmC* phase of M10/** will not be unwound. In such a case, ^{2}H NMR would provide an additional independent method to determine structural features, such as the tilt angle, and confirm the specific behaviour in the presence of external magnetic fields.

Acknowledgments

This work is supported by the Projects: ESF COST Action D35 WG0013-05, No. OC 175 from the Ministry of Education, Youth and Sports of the Czech Republic, No. IAA100100710 from the Grant Agency of the Academy of Sciences of the Czech Republic, No. 202/05/0431 and 202/09/0047 from the Czech Science Foundation, No AVOZ10100520 from the Academy of Sciences of the Czech Republic, by the Italian Ministry of Innovation, University and Research (MIUR) with the PRIN 2005 project. The authors gratefully acknowledge the German-Czech bilateral programme DAAD (German Academic Exchange Service)–ASCR (Academy of Science of the Czech Republic) D7-CZ8/08-09 and sincerely thank Professor Frank Giesselmann for the access to SAXS measurements.

References

[1] Kašpar M, Sverenyák H, Hamplová V, Glogarová M, Pakhomov S A, Vaněk P and Trunda B 1995 *Liq. Cryst.* **19** 775–8
[2] Kašpar M, Bubnov A, Hamplová V, Málková Z, Pirkl S and Glogarová M 2007 *Liq. Cryst.* **34** 1185–92
[3] Kašpar M, Hamplová V, Pakhomov S A, Stibor I, Sverenyák H, Bubnov A M, Glogarová M and Vaněk P 1997 *Liq. Cryst.* **22** 557–61
[4] Final report of EU FP5 project CP940168 1998 *Volume Stabilized Chiral Liquid Crystals for Display Applications* pp 1–106
[5] Lagerwall S T 1999 *Ferroelectric and Antiferroelectric Liquid Crystals* (Weinheim: Wiley–VCH)
[6] Lagerwall J P F and Giesselmann F 2006 *ChemPhysChem* **7** 20–45
[7] Lasertex, Wroclaw www.lasertex.com.pl
[8] Meyer R B, Liebert L, Strzelecki L and Keller P 1975 *J. Physique Lett.* **36** L69
[9] Blinc R 1975 *Phys. Status Solidi* b **70** K29
[10] de Gennes P G 1975 *The Physics of Liquid Crystals* (Oxford: Claredon)
[11] Romanov M V, Romanov V P and Val'kov A Y 2001 *Mol. Cryst. Liq. Cryst.* **359** 365–78
[12] Tordini G, Christianen P C M and Maan J C 2005 *Mol. Cryst. Liq. Cryst.* **435** 915–24
[13] Kopčanský P, Potočová I, Koneracká M, Timko M, Jadzyn J, Czechowski G and Jansen A M G 2003 *Phys. Status Solidi* b **236** 450–3
[14] Catalano D, Cifelli M, Domenici V, Fodor-Csorba K, Richardson R and Veracini C A 2001 *Chem. Phys. Lett.* **346** 259–66
[15] Domenici V, Veracini C A, Marini A, Zhang J and Dong R Y 2007 *ChemPhysChem* **8** 2575–87
[16] Chen A, Poon C D, Dingemans T J and Samulski E T 1998 *Liq. Cryst.* **24** 255–62
[17] Fung M 2002 *Prog. Nucl. Magn. Reson. Spectr.* **41** 171–86
[18] Domenici V, Geppi M and Veracini C A 2007 *Progr. Nucl. Magn. Reson. Spectrosc.* **50** 1–50
[19] Dong R Y, Geppi M, Marini A, Hamplova V, Kaspar M, Veracini C A and Zhang Z 2007 *J. Phys. Chem.* B **111** 9787–92
[20] Xu J, Dong R Y, Domenici V, Fodor-Csorba K and Veracini C A 2006 *J. Phys. Chem.* B **110** 9434–41
[21] Dierking I 2003 *Textures of Liquid Crystals* (Weinheim: Wiley–VCH)
[22] Fung B M, Khitrin A K and Ermolaev K 2000 *J. Magn. Reson.* **142** 97–101
[23] Maricq M M and Waugh J S 1979 *J. Chem. Phys.* **70** 3300–16
[24] Zhang J, Domenici V and Dong R Y 2007 *Chem. Phys. Lett.* **441** 237–44
[25] Nakai T, Fujimori H, Kuwahara D and Miyajima S 1999 *J. Phys. Chem.* B **103** 417–25
[26] Yoshizawa A, Kikuzaki H and Fukumasa M 1995 *Liq. Cryst.* **18** 351–8
[27] Metz G, Wu X and Smith S O 1994 *J. Magn. Reson.* A **110** 219–27
[28] Garic M, Obadovic D Z, Bubnov A, Hamplová V, Kašpar M and Glogarová M 2004 *Mol. Cryst. Liq. Cryst.* **412** 587–96
[29] Piecek W, Raszewski Z, Perkowski P, Przedmojski J, Kedzierski J, Drzewinski W, Dabrowski R and Zielinski J 2004 *Ferroelectrics* **310** 125–9
[30] Skarp K, Flatischler K and Lagerwall S T 1988 *Ferroelectrics* **84** 183–95
[31] Carlsson T, Zeks B, Filipic C and Levstik A 1990 *Phys. Rev.* A **42** 877–89
[32] D'Have K, Rudquist P, Lagerwall S T, Pauwels H, Drzewinski W and Dabrowski R 2000 *Appl. Phys. Lett.* **76** 3528–30
[33] Bubnov A, Kašpar M, Novotná V, Hamplová V, Glogarová M, Kapernaum N and Giesselmann F 2008 *Liq. Cryst.* **35** at press
[34] Goodby J W, Stanley A J, Both C J, Nishiyama I, Vuijk L D, Styring P and Toyne K J 1994 *Mol. Cryst. Liq. Cryst.* **243** 231–98
[35] Zhang J, Ferraz A, Ribeiro A C, Sebastiao P J and Dong R Y 2006 *Phys. Rev.* E **74** 061704
[36] Cifelli M, Domenici V and Veracini C A 2005 *Mol. Cryst. Liq. Cryst.* **429** 167–79